

Design and Construction of Tsurumi Tsubasa Bridge Superstructure

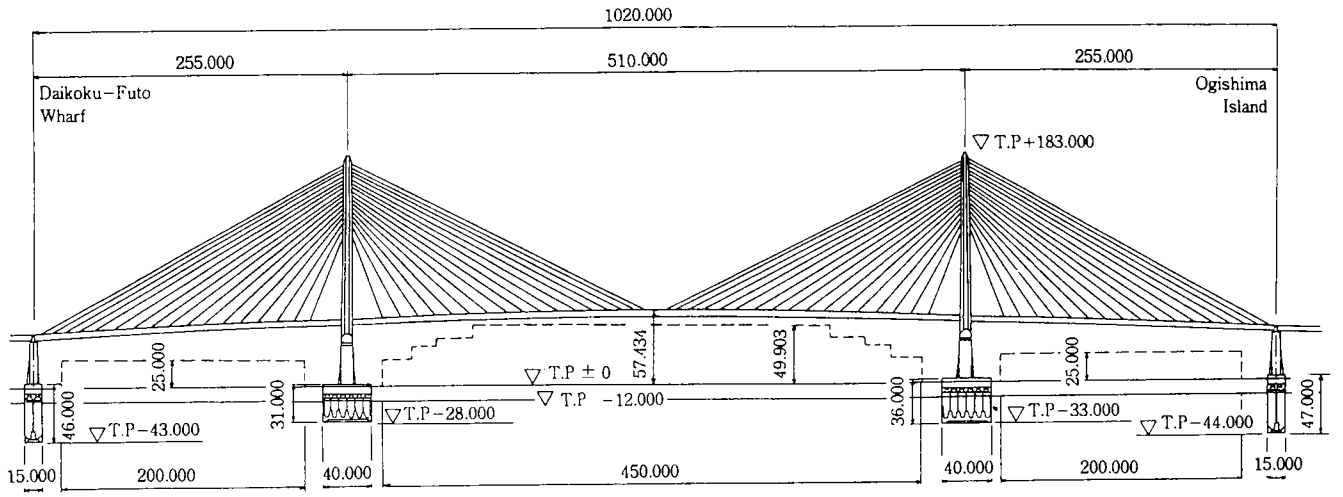
Mamoru Enomoto, Hisashi Morikawa, Haruo Takano, Masafumi Ogasawara, and
Hiroyuku Hayashi, *Metropolitan Expressway Public Corporation, Japan*
Wataru Takahashi, *Miyaji Iron Works Co., Ltd., Japan*
Nobuo Watanabe and Masahito Inoue, *NKK Corporation, Japan*

The Tsurumi Tsubasa Bridge is a single-plane, three-span continuous cable-stayed bridge 1020 m long, with a 510-m center span. It was constructed over the Tsurumi Fairway, which lies between the Daikoku-Futo Wharf and Ogishima Island in Yokohama. The total weight of the steel superstructure is about 38,000 tons with the foundation built on pneumatic caissons. This bridge was built for the Metropolitan Expressway. In the future, National Highway 357 will cross the Tsurumi Fairway on a separate bridge built parallel to and in the same style as the Tsurumi Tsubasa Bridge. Therefore, the appearance and the earthquake and wind resistance of the Tsurumi Tsubasa Bridge were studied not only with consideration being given to the first but also the second bridge standing parallel to the first. As for the construction of this new bridge, at each step of construction actual values were checked against design values to ensure safety and precision. Construction was accomplished with a high degree of precision, owing to the introduction of a precision control system.

The Tsurumi Tsubasa Bridge, a 1020-m-long, single-plane, three-span continuous cable-stayed bridge with a 510-m center span, was constructed over the Tsurumi Fairway, which lies between the Daikoku-Futo Wharf and Ogishima Island in Yo-

kohama. The total weight of the steel superstructure is about 38,000 tons. Pneumatic caisson foundations were used. The general view is shown in Figure 1. This bridge was built for the Metropolitan Expressway. In the future, National Highway 357 will cross the Tsurumi Fairway on a separate bridge built parallel to and in the same style as the Tsurumi Tsubasa Bridge. Therefore, the appearance and the earthquake and wind resistance of the Tsurumi Tsubasa Bridge were studied with consideration being given not only to the first but also the second bridge parallel to the first.

Photomontage and computer graphics techniques were used to study the projected appearance of the two bridges standing parallel. The study revealed that with a double-plane, cable-stayed bridge design, the cables of the two bridges would appear to be entangled and that with a two-leg-type lower tower, the two pair of legs would appear to be intermingled. Therefore, a single-plane semi-fan-type cable arrangement was adopted. The lower part of the tower was designed as a concrete wall construction with an octagonal cross section, and the upper tower was configured as an inverted Y-shape with a trapezoidal cross section. To the extent possible, the block joints were welded at the construction site to provide a smooth, slender appearance.



T.P. :Standard mean sea level of Tokyo Bay

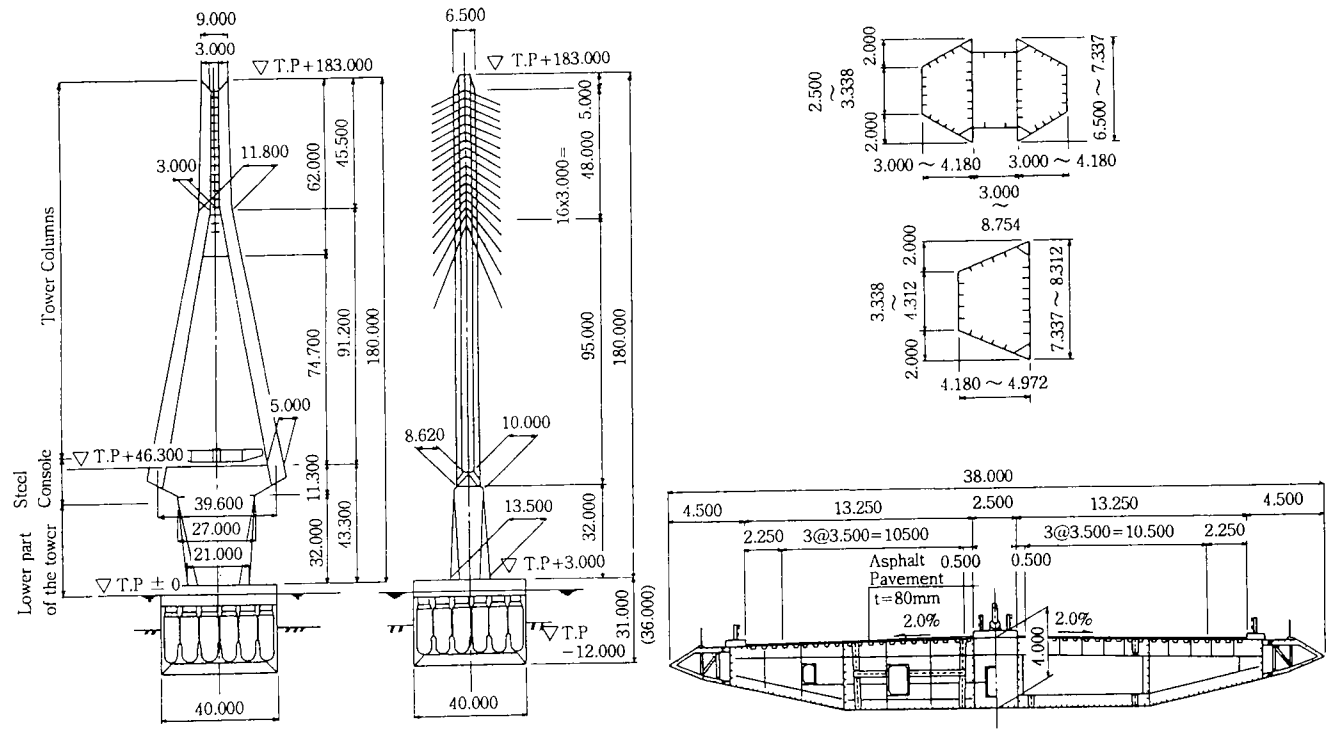


FIGURE 1 General view.

Because it stands in the sea, the concrete lower part of the tower was coated with a fluorine-containing resin to provide excellent durability and appearance. The color is white (N.9.5) to enhance its appearance in the blue of the sky and sea. An artist's conception of the twin bridges is shown in Figure 2.

The girder has a total width of 38 m, including fairings. It has a five-cell box section with a height of 4 m to increase torsional rigidity because the bridge has a single-plane, cable-stayed deck with very long spans.

Because the section is wide, a bending moment occurs in the transverse direction of the girder, and compressive stresses act on the lower flange in the spans and on the deck plate at the support points. Therefore, local and total buckling were studied for the members on which compressive stresses act in two directions (transverse and longitudinal). Verification was performed by three-dimensional finite-element method (FEM) analysis because stresses concentrate in the supports and at the cable anchoring sections. The maximum deflection of

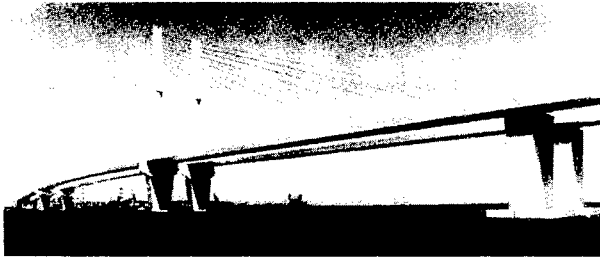


FIGURE 2 Artist's conception of the twin bridges.

the girder caused by live load (including the torsion-induced vertical displacement of the road shoulder) is $\delta = 853$ mm. Vertical displacement of the road shoulder caused by a one-sided live load is $\delta = 467$ mm and produces the largest torsion angle ($\phi = 0.0123$ rad). Under normal conditions, however, the torsion angle is not so large.

The lower tower starts at the upper caisson slab and includes the steel console, which supports the girder and tower column. To smoothly transmit the load from the tower column and girder to the caisson foundation, a design was adopted that used a steel-frame reinforced concrete structure to about 20 m above the upper slab of the caisson foundation and a concrete steel multicell and steel console above it. The basic design concept was for the compressive force of the steel multicell section to be completely transferred to the concrete by a bearing plate and for the tensile force occurring during an earthquake to be borne by the steel frame. However, it was suspected that the total load could not be transferred by the bearing plate and, clearly, tensile force will flow to the reinforced concrete from the steel cell-plate structure. Dowels (D22 steel bars passing through holes cut in the steel cell plate) are used to provide a tensile load path between the steel cell-plate structure and the concrete and to permit smooth transfer of load. An experiment was performed using a large model to confirm the feasibility of these dowels. From the experiment, it was assumed in the design that 50 percent of the compressive force would be transferred from the bearing plate to the concrete and the remainder would be transferred through the dowels. The structure of the lower part of the tower is shown in Figure 3.

The tower column was made somewhat higher to reduce the deflections caused by the live load and the variations in cable tension. The tower height from the top of the foundation was set at 180 m. The tower column is subjected to high axial force and bending moment, and stresses concentrate at the cable anchoring locations and at the branch. Therefore, verification was performed by three-dimensional FEM analysis. Seismic resistance and elastic buckling analyses were carried out

to confirm the stability of the structural system of the whole tower column.

The cables were arranged as a semifan with 17 stay cables. The cables are nongrout-type parallel wire strands (PWS) that are made by bundling galvanized wires 7 mm in diameter and coating with polyethylene. The cable arrangement was studied using cables with 499 wires (coated outside diameter, 192 mm; unit weight, 156.8 kg/m), which is the maximum size that could be used in terms of production, transportation, and installation. Of the 34 cables attached to each tower 15 are maximum section cables. The cable tension was adjusted so that a dead load bending moment was not induced on the tower. A saddle-type cable anchorage was used on the tower side, whereas anchorage girders were used on the girder side. After the cable was anchored to the saddle on the tower, the girder end was pushed inside the girder into the anchorage girder from the upper side.

Attaching horizontal cables, set in the girder, were installed to restrain the relative horizontal displacement between the girder and tower. This is because the link structure increases the width of the tower and affects the clearance between the twin bridges and because oscillation of the girder must be restrained because of its low bending rigidity. The attaching horizontal cables were also made from PWS. Four 117-m cables are attached to each tower: two cables on the center span and the others on the side spans. Each cable has 367 wires and a coated diameter of 167 mm. The initial cable tension of 690 tons-force per cable was chosen to permit it to be maintained by the combination of live load and temperature change and to ensure that it did not exceed the allowable value during an earthquake.

Two vane-type dampers were installed on the tower steel console to help dampen longitudinal oscillation of the girder. The vane-type damper converts horizontal motion to rotational motion and is constructed so that flow is resisted when oil inside its left and right pressure chambers passes through orifices in the partition. This resistance induces a horizontal reaction in proportion to the square of the relative velocity of the girder and tower. To maintain the horizontal reaction at a fixed value above a certain relative velocity, a pressure control valve is installed in the partition. The vane-type damper scarcely resists low-speed motion such as the expansion and contraction of the girder caused by temperature changes. Results of the seismic response computations for the performance of these dampers in concert with the attaching horizontal cables indicate that, during an earthquake, they reduce horizontal displacement of the girder by about 30 percent and cable tension by 20 to 30 percent from the levels reported when only attaching horizontal cables are used. As a result, the attaching horizontal cables are kept in tension, re-

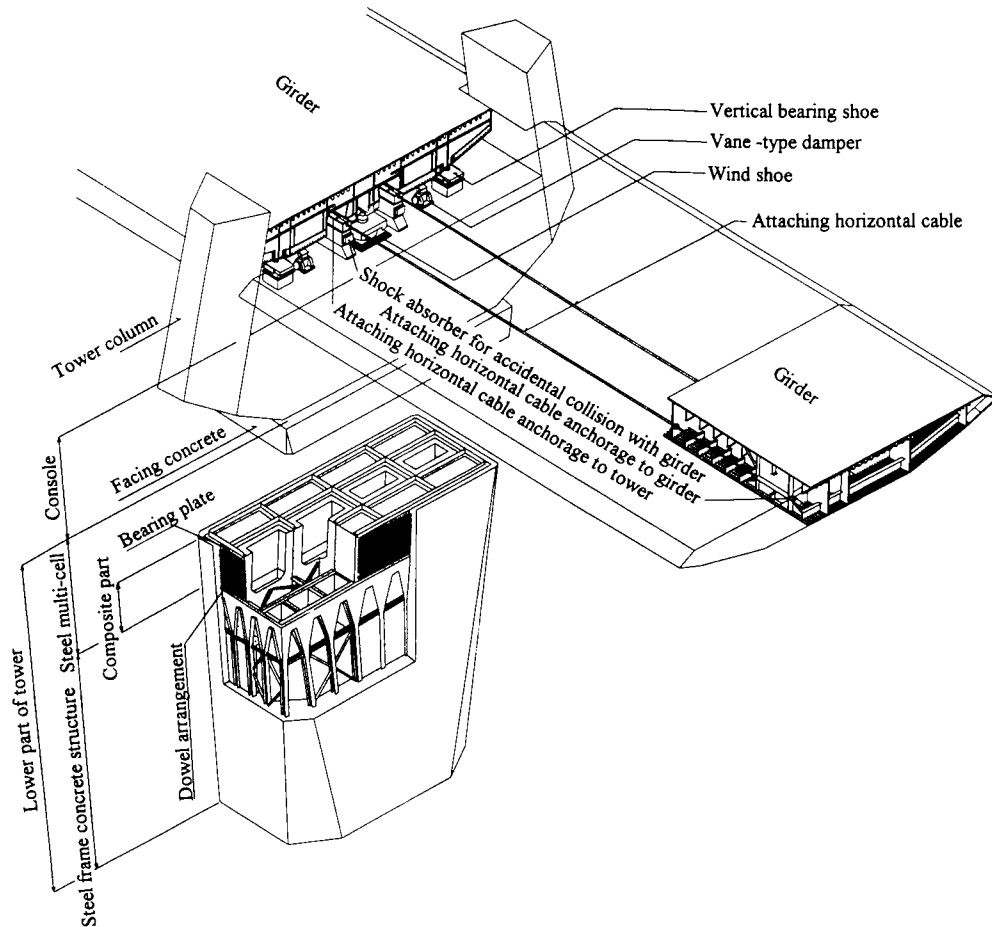


FIGURE 3 Structure of the lower part of the tower.

sulting in increased safety. The mechanism and the reaction properties of the vane-type damper are shown in Figures 4 and 5.

The span ratio between the side spans and the center span is approximately 1:2. Therefore, there is almost no vertical dead load reaction at the end supports, and both positive and negative reactions caused by the live load continually and repeatedly act on the pendulum supports of the end pier. Under normal conditions ($1/2$ of the standard live load), the pendulum supports should be in compression at all times. To ensure this compression, 920 tons-force (about 250 m^3) of concrete was poured inside the girder ends.

Two vertical bearing supports, one horizontal bearing support, two attaching horizontal cable anchorage systems, and two vane-type dampers were mounted on the tower. Two pendulum supports and one horizontal bearing support were mounted at the girder end.

Vortex shedding and wind/rain-induced vibration of the cables were often observed during the erection of the Tsurumi Tsubasa Bridge. To suppress these vibrations, both oil and (high damping) rubber dampers were

applied to the stays at the deck level. The rubber is especially effective not only in suppressing the vibration but also in reducing the additional stress caused by the live load. From the aesthetic point of view, these apparatuses were set at the same height as the handrail. The structure is shown in Figure 6.

STUDY OF EARTHQUAKE RESISTANCE

Magnitude of Earthquake and Incident Seismic Wave

On the basis of a survey of past major earthquakes, the expected value of the magnitude M of an earthquake with a return period of 75 years at the location of the Tsurumi Tsubasa Bridge was calculated as $M = 7.8$ to 8.2 with an epicenter between 50 and 200 km away. To establish the acceleration response spectrum of the seismic waves on the bedrock (the target spectrum of the seismic waves on the bedrock), earthquake observation records for the Daikoku-Futo Wharf during the past 10

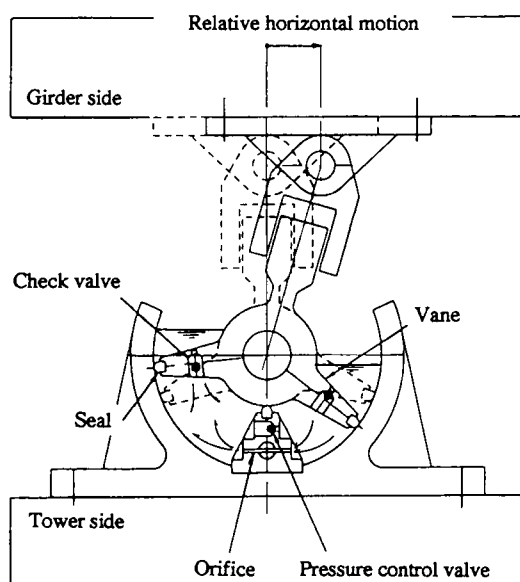


FIGURE 4 Vane-type damper mechanism.

years and other observed earthquakes were used as references. Artificial seismic waves were created that correspond to this target spectrum. The design acceleration spectrum is shown in Figure 7; the artificial seismic wave is shown in Figure 8.

Analysis Model

Artificial seismic waves were applied to the bedrock. The dynamic characteristics (shear rigidity and damping ratio) were obtained by using the theory of wave superimposition (SHAKE), and a time-history response analysis was performed using a simplified three-dimensional FEM model. The reflection of waves (box effect) in the zone being analyzed, which is caused by treating the subsoil as a continuous, semi-infinite body in a finite zone, was considered using a simplified three-dimensional FEM model. Also, dissipation of the wave energy outside of the zone was considered by establishing the transfer and viscosity boundaries. The simplified three-dimensional model is shown in Figure 9.

Earthquake-Resistant Design for Foundation Structure

The results of the dynamic analyses using the simplified three-dimensional FEM model indicated that there was a dynamic interaction between the foundation and the subsoil and that subsoil displacement mainly acts on the caisson foundation. This subsoil displacement was evaluated as a horizontal load in the static design.

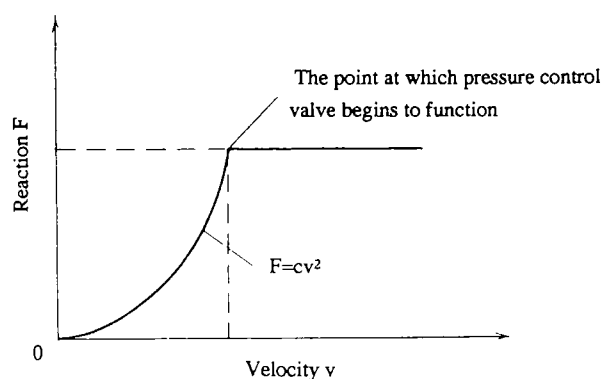


FIGURE 5 Reaction properties of vane-type damper.

Earthquake-Resistant Design for Superstructure

The time history response analysis for the superstructure was performed by using a lumped mass model. A problem of this model is defining the strength and damping characteristics of the subsoil spring that models the connection of the foundation to the subsoil. These values were made equivalent to the results of the simplified three-dimensional FEM analysis. The time history response analysis using the lumped mass model was used to check the design, and the response spectrum method was used to do design computations. The distributions of bending moment of the towers do not match if a superstructure model is used that fixes the bottom ends of the towers, and a horizontal acceleration response spectrum is used for the top of the foundation. This is because the effect of rotation of the foundation is not included in the calculation. Therefore, the response spectrum method was used by extending the model down to the bottom of the foundation.

WIND RESISTANT DESIGN

Design Wind Velocity

The design wind velocity was determined from the 100-year return expected value calculated from 10-min average wind velocity observations over the 55-year period since 1928 by the Yokohama Meteorological Observatory and over the past 4 years from the tower of the Daikoku Bridge, which is near the location of the proposed Tsurumi Tsubasa Bridge (girder, $V_z = 53.0$ m/sec; tower and cable, $V_z = 58.0$ m/sec).

Wind Tunnel Tests

Wind tunnel tests were performed on the completed bridge, the cantilevered erection of the girder, and the

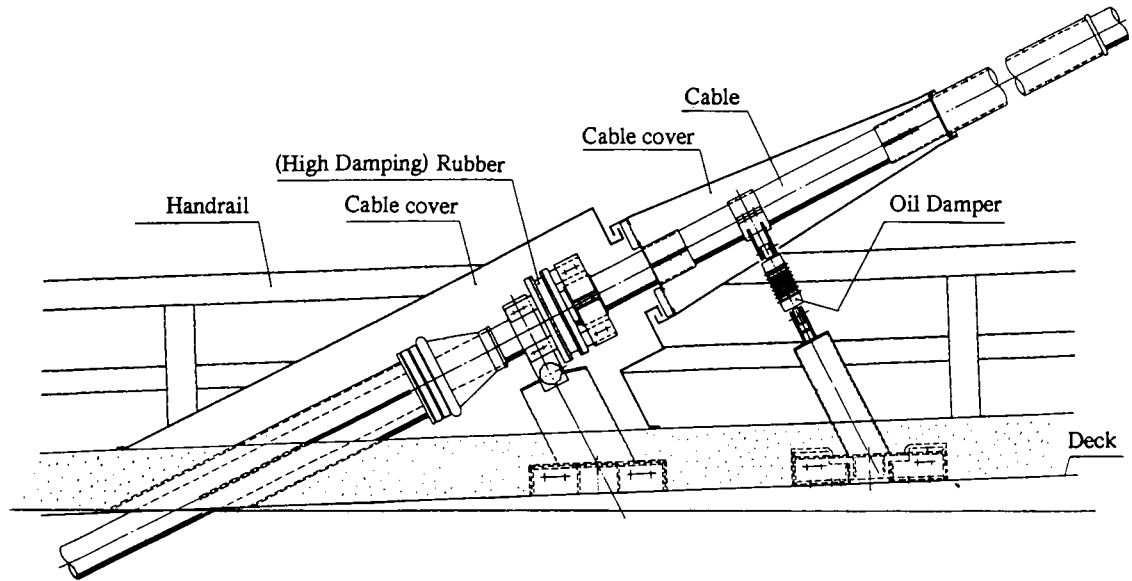


FIGURE 6 Cable damper.

erection of the tower. Tests were performed on the two-dimensional, spring-supported girder sectional model for attack angles of 0 degree and +3 degrees. The flutter wind velocity in the test of the single bridge model was far higher than the design wind velocity, and harmful vibrations did not occur at wind velocities up to 100 m/sec. The effectiveness of 2-m fairings attached to both edges of the girder was demonstrated. However, in the test of the twin bridge model, self-excited vibrations occurred at wind velocities of 69 to 72 m/sec. To increase

the flutter wind velocity, blocking of the medial strip guard fence (i.e., constructing a center barrier) was tried. This measure increased the flutter wind velocity above the design wind velocity of $V_F = 74.4$ m/sec.

In the completed bridge model test, a test that is similar to that used on the girder sectional model was performed to check the effect of the center barrier. Flutter or other harmful vibrations did not occur regardless of the presence of the center barrier in the test of the single bridge model. The response characteristic of the test of

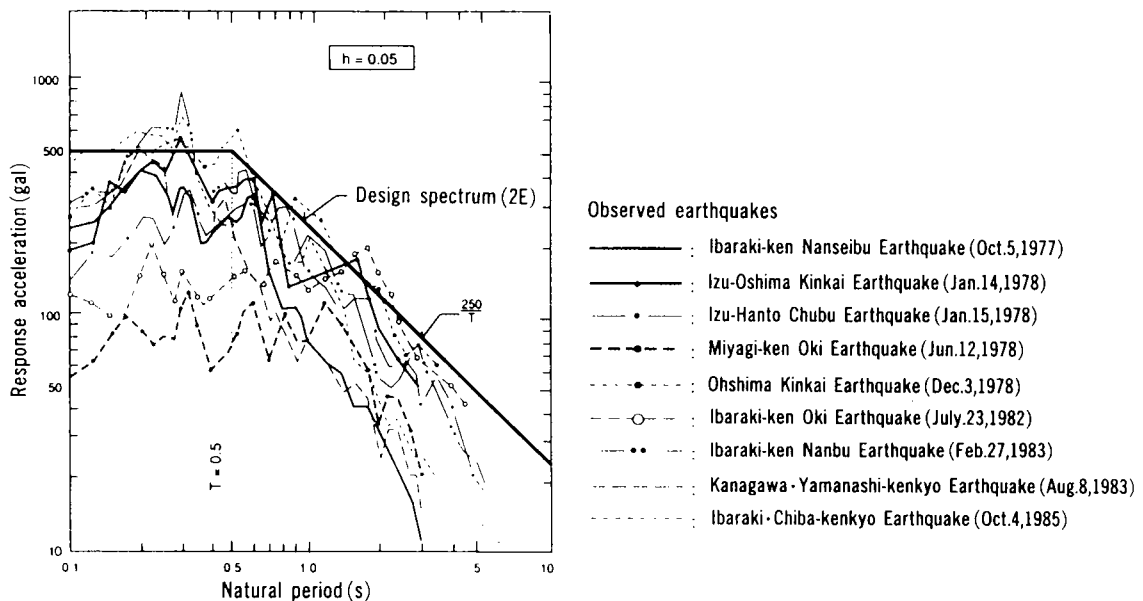


FIGURE 7 Design acceleration spectrum.

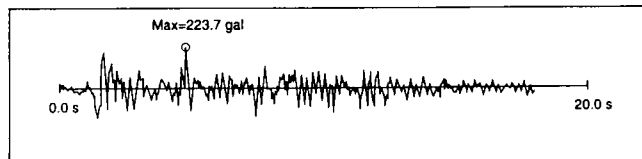


FIGURE 8 Artificial seismic wave.

the twin bridge model was almost the same as that of the single bridge model. In the uniform flow test flexural vibration did occur. However, this was prevented by the installation of the center barrier. It is therefore thought that a center barrier need not be installed as long as the bridge stands alone, but that it should be installed when the second bridge is built.

At an early stage of the design project, the tower column section was to be rectangular, and the occurrence of galloping was expected on the basis of preliminary test results. However, galloping was prevented by changing the cross section to a trapezoidal section.

ERECTION OF THE SUPERSTRUCTURE

Erection of the Foundation of the Tower

After the steel frames for the lower parts of the towers were assembled into single units on land, they were divided into top and bottom halves, carried to the site by

a 700-ton floating crane, and installed in the top slab of the caissons. Next the steel multicell located below the console bottom was erected, reinforced concrete was poured inside and outside of the steel multicell, and the whole composite was integrated into a single unit by the dowels, which were already set in place on the steel multicell. Finally, the steel consoles were erected as a single unit with a 3,500-ton floating crane.

Erection of the Tower and the Girder

The construction stages are outlined in Figure 10. The girders of the side spans were divided into three large blocks. After two vents were set for the side spans, the girders were erected in large blocks by a 3,500 ton floating crane. The middle parts of the tower were constructed as large blocks by a 3,500 ton floating crane, and the upper parts of the tower were constructed by raising a single block by means of a 650-ton crawler crane set on the girder deck. They were then welded. Because vortex excitation occurred during erection of the tower column, measures were taken by installing a tuned mass damper device.

The tower side 115-m portions of the center span girder were supported by vents set approximately 80-m from the towers in the center span. These girder portions were erected in large blocks by a 3,500-ton floating crane. To permit the bridge to extend over the Tsurumi Fairway, approximately 240 m of the girder in the central portion of the center span was erected using the cantilever-type erection method in which the girder

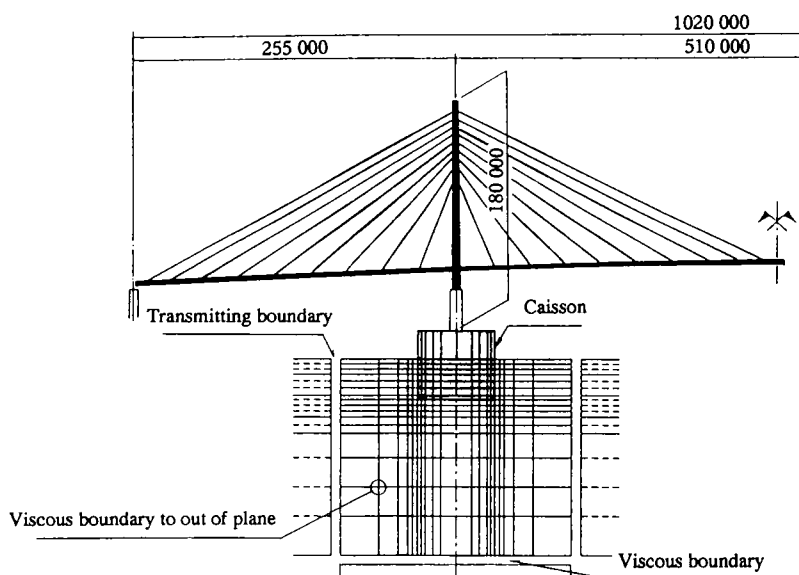


FIGURE 9 Simplified three-dimensional model.

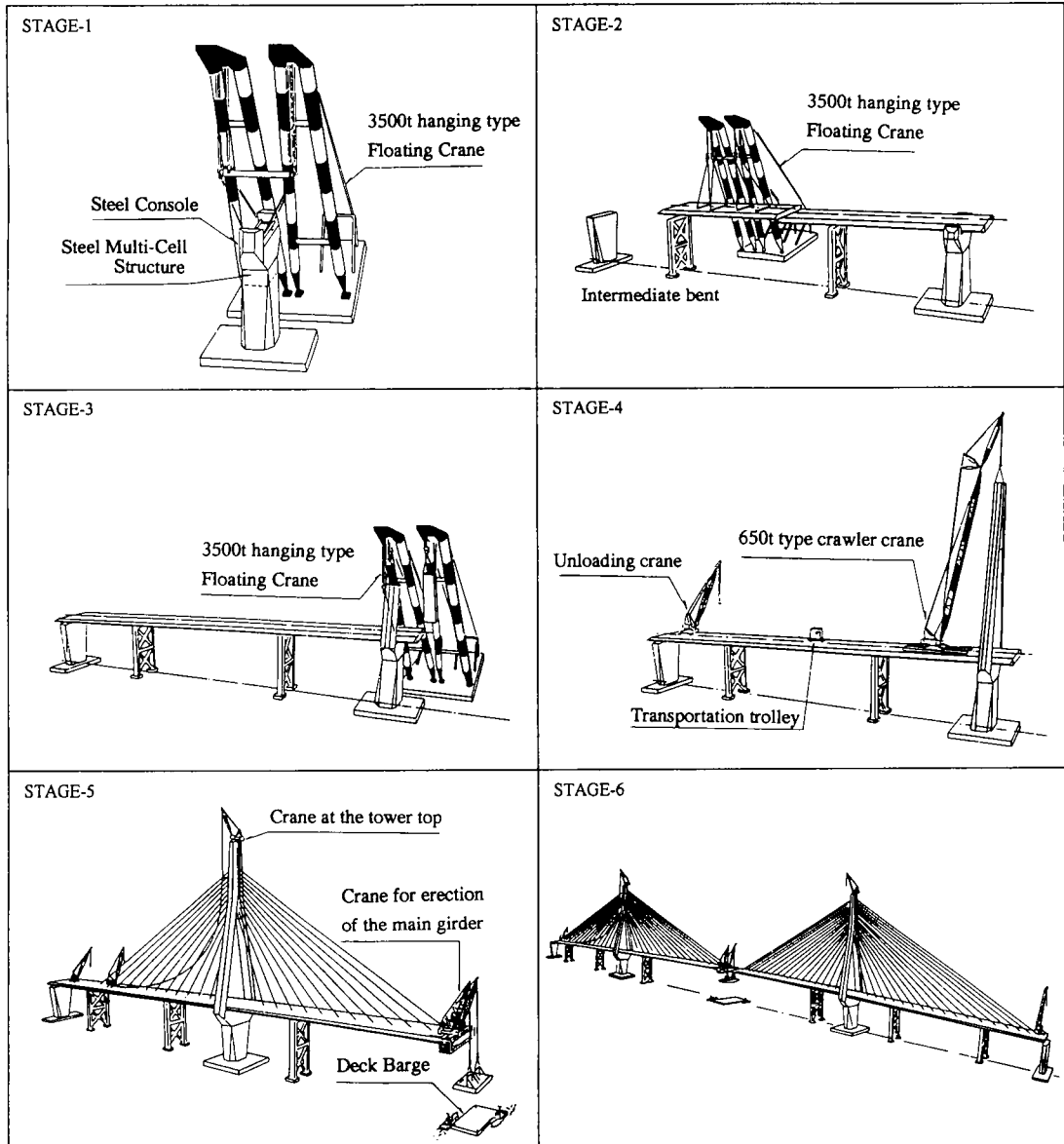


FIGURE 10 Construction stages.

was gradually extended from both sides as the cables were installed and tensioned—a method that took advantage of the mechanical characteristics of cable-stayed bridges. This method made it easy to control the process precisely, and procedures could be hastened at the site. Toward this aim, deck barges transported blocks of girder to a location directly below the place where they were to be installed, and they were raised to bridge level by 450 ton crawler cranes mounted on each side of the girder tips. Center-span girder closure was performed by using the cranes to raise the girder closure blocks to the correct position in the same manner as that for other blocks and then splicing both ends.

Installation of Cables

The cable was unreeled on the deck, and the tower side end was lifted by a crane set on top of the tower. After it was anchored to the saddle on the tower, the girder side end was pushed inside the girder into the anchorage girder from the upper side.

Precision Control During Construction

In the case of a cable-stayed bridge, deviation of stress and dimensions from the design values can be adjusted as the distance between fixed points can be changed by

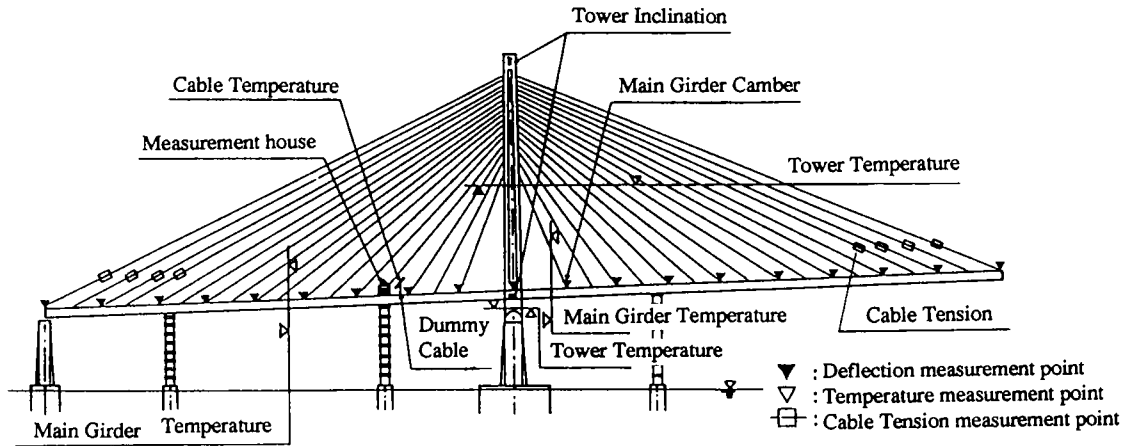


FIGURE 11 Arrangement of the measurement instruments.

means of shim plates installed at fixed points on the cables. To ensure safety during construction and high precision at completion, a computerized precision control system was applied.

As a preparation before the shim adjustment work, a calculation model was formed on the basis of the various errors and construction methods, and control limit values and influence values of shim plate thickness and temperature on cable tension and deformation were evaluated by analytic calculation, which was processed by a computer.

On the day of shim adjustment work, construction loads (mainly those on the bridge surface) were to be surveyed, and the resultant load data were input into the computers for precision control at the construction site linked with a central computer, and detailed control calculations were conducted. After confirmation that nighttime temperatures at each part of the bridge had been stabilized, measurements were taken. Vibration frequency of the cable was measured by an acceleration meter, the main girder camber was measured by level meter (communicating tube), and tower inclination was measured by laser level. These measurements were controlled by the centralized control system through com-

puters at the construction site. The arrangement of the measurement instruments is shown in Figure 11.

Conversion of the cable vibration frequency into tension and the temperature correction were processed by the computer. Measured data were transmitted to precision-control personal computers, which calculated optional solutions for shim adjustment by the least-squares method and expected values for any shim adjustment of choice. According to input data and control values, the final shim value for actual use was decided in reference to these computer calculations.

After shim adjustment work, if the comparison of measured values and control values mentioned earlier gave good results, the work for the day was finished, and work on the next step started the following day. Because of the introduction of the precision control system, construction was accomplished with the precision of half the control limit values. Control items and results of the precision control are shown in Table 1.

SUMMARY

An outline of the design and construction of the superstructure for the Tsurumi Tsubasa Bridge has been pre-

TABLE 1 Control Items and Result of Precision Control

	Control Limit Value	Control Target Value	Results
Main Girder Camber	$\pm [25+(L-40)]*0.5$ (L: Span Length) Center Span $\delta = \pm 240\text{mm}$ (L=510m) Side Span $\delta = \pm 120\text{mm}$ (L=255m)	1/2 of the Control Limit Value	Center Span $\delta = +114\text{mm}$ Side Span $\delta = -58\text{mm}$
Tower Inclination	1/2000 of the Tower height $\delta = \pm 180000/2000 = \pm 90\text{mm}$	1/2 of the Control Limit Value	$\delta = -10\text{mm}$
Cable Tension	$\pm \text{allowable Tension} - \text{Design Tension} $	1/2 of the Control Limit Value	$\Delta T = -55 \sim 78\text{t}$

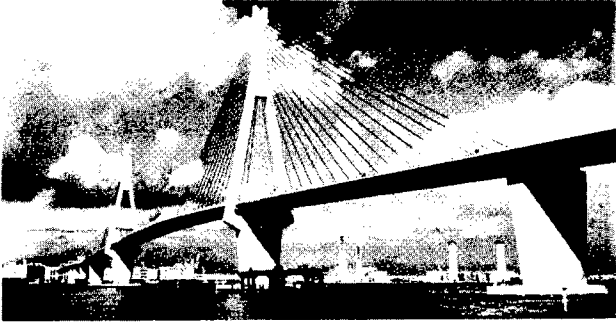


FIGURE 12 Tsurumi Tsubasa Bridge.

sented. The Tsurumi Tsubasa Bridge, which was completed at the end of 1994 as a result of the introduction of much new technology, is shown in Figure 12.

ACKNOWLEDGMENT

The Investigation and Research Committee Regarding the Design and Construction of the Tsurumi Tsubasa Bridge (Chairman, Manabu Ito of the University of Tokyo) was established to study technical questions in carrying out this project. The authors wish to thank those concerned with the design and construction of the Tsurumi Tsubasa Bridge, including the members of the committee.